Chemical Science

ROYAL SOCIETY OF CHEMISTRY

EDGE ARTICLE

View Article Online
View Journal

Check for updates

Cite this: DOI: 10.1039/d5sc03449c

All publication charges for this article have been paid for by the Royal Society of Chemistry

Received 13th May 2025
Accepted 2nd July 2025

DOI: 10.1039/d5sc03449c

rsc.li/chemical-science

Manganese-mediated C(sp)–Si cross-electrophile coupling of alkynyl halides with chlorosilanes†

Quan Lin, Liping Lin, Jingjing Wang, Daohong Yu, * Zhengwang Chen * and Zhong-Xia Wang *

We present a manganese-mediated cross-electrophile coupling (XEC) that directly constructs C(sp)–Si bonds between alkynyl halides and chlorosilanes. By leveraging manganese as a reductant, this method enables a mild and operationally simple approach. Mechanistic studies reveal the *in situ* generation of key intermediates alkynylmanganese in amide media, which undergo S_N2 substitution with chlorosilanes to afford diverse alkynylsilanes in high yields (up to 99%) with suppressed diyne byproducts. To our knowledge, this is the first discovery of alkynylmanganese species, derived from readily available alkynyl halides, for C(sp)–Si cross-electrophilic coupling. This work expands the scope of XEC in organosilicon chemistry and provides a robust alternative for C(sp)–Si bond formation.

Introduction

Cross-electrophile coupling (XEC) has emerged as a transformative strategy for C–C bond formation, holding considerable potential across diverse disciplines including pharmaceutical chemistry, materials science, and natural product synthesis.[1] The XEC protocol achieves direct coupling of two electrophilic substrates *via* transition-metal catalysis under reductive conditions, exhibiting exceptional substrate compatibility while eliminating preformed organometallic reagents over conventional cross-coupling approaches.[2] Beyond its well-established C–C coupling, XEC has recently demonstrated notable progress in the coupling of carbon electrophiles with commercial chlorosilanes as an indispensable strategy for constructing C–Si bonds, spanning C(sp^3)–Si and C(sp^2)–Si architectures, as evidenced by pioneering contributions from Shu and Oestreich, and others (Fig. 1a).[3] Huang's recent report of a cobalt-catalyzed XEC reaction that couples pre-synthesized alkynyl sulfides with chlorosilanes to access C(sp)–Si alkynylsilanes represents a significant advancement (Fig. 1b, top).[4] Nevertheless, the direct cross-coupling of readily available alkynyl halides with chlorosilanes to construct C(sp)–Si bonds has remained unreported.

Three fundamental challenges could persist in C(sp)–Si XEC reactions involving alkynyl halides and chlorosilanes. First, the high reactivity of alkynyl halides often results in undesired homocoupling and addition side reactions.[5] Second, the low reactivity and elevated bond dissociation energy (BDE) of R_3Si–Cl bonds (*ca.* 117 kcal mol^{-1}),[6] compared to R_3C–Cl bonds (*ca.* 84 kcal mol^{-1}),[7] adversely affect the XEC reactivity of alkyne electrophiles. Third, the diminished nucleophilicity of

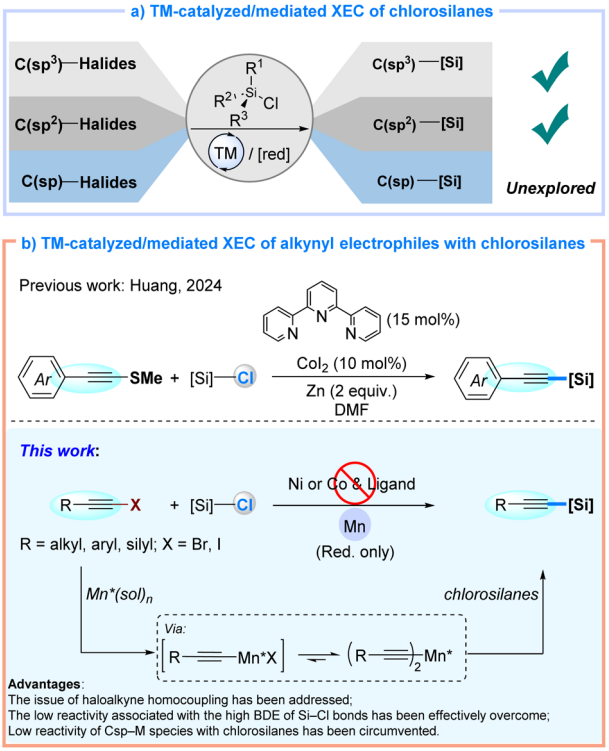

Fig. 1 Cross-electrophile C–Si coupling reactions.

Jiangxi Provincial Key Laboratory of Synthetic Pharmaceutical Chemistry, College of Chemistry and Materials Science, Gannan Normal University, Ganzhou 341000, P.R. China. E-mail: yudh@gnnu.edu.cn; chenzwang2021@163.com; zhongxiawang@ncu.edu.cn

† Electronic supplementary information (ESI) available: Synthetic details, spectroscopic characterization and crystallographic data. CCDC 2423603. For ESI and crystallographic data in CIF or other electronic format see DOI: https://doi.org/10.1039/d5sc03449c

commonly reported C(sp)–Ni/Co intermediates, relative to aryl or alkyl-Ni/Co species, further reduces their reactivity toward chlorosilanes.[3a,8] Therefore, developing an efficient cross-electrophilic coupling protocol for the direct synthesis of alkynylsilanes from alkynyl halides is both timely and essential.

Herein, we report a manganese-mediated XEC reaction that enables direct C(sp)–Si bond formation between alkynyl halides and chlorosilanes. This method innovatively employs metal manganese as a reductant, circumventing requirements for sophisticated catalytic systems involving transition-metal catalysts and organic ligands. Notably, mechanistic investigations reveal the *in situ* generation of intermediate alkynylmanganese species from alkynyl halides as precursors in the presence of manganese metal and amide solvent, followed by S_N2 nucleophilic substitution reactions with chlorosilanes.[9] This protocol enables the synthesis of a variety of alkynylsilanes in high yields (up to 99%) under mild conditions, effectively suppressing the formation of diyne byproducts (Fig. 1b, bottom). As such, this discovery establishes an alternative synthetic toolkit for organosilicon chemistry.

Results and discussion

We initiated our studies by evaluating the coupling reaction between alkynyl bromide **1a** and chlorosilane **2a** (Table 1). Following extensive optimization, we identified the optimal combination of Mn (3 equiv.) in dimethylacetamide (DMA) (0.15 mol L^{-1}), which produced the desired product **3a** with an isolated yield of 80% within a reaction time of 2.5 hours (Table 1, entry 1). The addition of catalytic amounts of $NiBr_2$(dtbbpy) or $CoBr_2$/Terpy under these conditions notably reduced the yields, resulting in 23% and 3% of the desired alkynes, and 57% and 29% of diynes, respectively (Table 1, entries 2 and 3). The reaction did not proceed in the absence of Mn, nor when the organic reductant TDAE was used as a substitute (Table 1, entries 4 and 5). Alternative metal reductants, aside from iron, were capable of yielding the target product, albeit with lower yields; magnesium specifically may facilitate the formation of the alkynyl Grignard reagent (Table 1, entries 6–8). Amide solvents are essential for the success of this reaction, with DMA exhibiting particularly favorable properties (Table 1, entries 1 and 9–13). Under an air atmosphere, the reaction yielded only 22% of product **3a**, alongside 29% of side product **3a′** (Table 1, entry 14). Furthermore, upon introducing D_2O (1.0 equivalent) into the reaction conditions, the formation of **3a** was inhibited, yielding 23% of deuteryne (Table 1, entry 15). These findings further support the presence of an organomanganese intermediate.[2a,10] Additionally, we performed a gram-scale synthesis of **3a**, achieving a yield of 64%, thereby underscoring the robustness of this protocol and its potential for synthetic applications (Table 1, entry 16).

Under optimized reaction conditions, we undertook an initial exploration of the scope of alkynyl bromides and representative alkynyl iodides in this manganese-mediated XEC utilizing TMSCl, $VinylMe_2SiCl$, or VinylPhMeSiCl. The unactivated alkynyl halides exhibited significant reactivity with chlorosilanes, producing target products in yields ranging from 31% to 87%. Both silicon- and alkyl-substituted alkyne halides demonstrated compatibility within this reaction system (Fig. 2, products **3b–3f**). Notably, tertiary alkyl-substituted alkynyl bromides (**3f**) exhibited significantly higher reactivity than secondary alkyl counterparts (**3e**), whereas primary alkyl-substituted alkynyl bromides (**3c**, **3d**) required elevated amounts of chlorosilane and manganese, along with prolonged reaction times, to achieve complete conversion. We postulate that primary alkyl-substituted alkynyl bromides exhibit relatively low steric hindrance at the propargylic position may drive substrate isomerization to the allenic form, thereby inhibiting the formation of the alkynylmanganese species and enabling substrate recovery.[11] Subsequently, we examined the scope of aromatic alkynyl halides (**3g–3y**). Remarkably, alkynylferrocene (**3g**) and alkynylbiphenyls (**3h–3i**) were found to be compatible with the standard conditions, yielding moderate results. The products **3j–3l** indicate that aromatic alkynyl halides containing electron-donating groups (EDGs), such as methoxy and alkyl substituents on the benzene ring, are still able to yield the desired products in moderate to good yields. Similarly, the presence of electron-withdrawing groups (EWGs) such as $–CO_2Me$ (**3m**), $–CO_2Ph$ (**3n**), and $–CF_3$ (**3o**) on the benzene ring produced comparably favorable outcomes. The reaction also exhibits excellent chemo-selectivity; we performed the XEC with alkynyl bromides containing various active functional groups, synthesizing products such as bromobenzene (**3p**), benzonitrile (**3q**), and benzaldehyde (**3r**) in yields ranging from 42% to 91%,

Table 1 Optimization of reaction conditions[a]

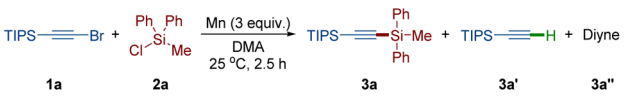

Entry	Variation	Yield (%) 3a	3a′	3a″
1	None	86 (80)[b]	6	0
2	w/ $NiBr_2$(dtbbpy) (10 mol%)	Trace	23	57
3	w/ $CoBr_2$ & Terpy (10 mol%)	23	3	29
4	w/o Mn	0	0	0
5	TDAE instead of Mn	0	0	0
6	Mg instead of Mn	64	12	0
7	Zn instead of Mn	25	25	0
8	Fe instead of Mn	0	0	0
9	DMF instead of DMA	52	15	0
10	THF instead of DMA	0	Trace	0
11	Toluene instead of DMA	0	0	0
12	DMSO instead of DMA	0	Trace	0
13	CH_3CN instead of DMA	0	Trace	0
14	Under air	22	29	0
15	1.0 equiv. D_2O was added	25	23[c]	0
16	4 mmol of **1a** (gram scale)	64[b]	8	0

[a] Standard conditions: **1a** (0.15 mmol), **2a** (0.45 mmol), Mn (0.45 mmol), DMA (1 mL), 25 °C, Argon, yields were determined by GC using dodecane as the internal standard. [b] Isolated yield. [c] Deuterated product. TDAE = tetrakis(dimethylamino)ethylene. Terpy = 2,2′:6′,2″-terpyridine. w/ = with. w/o = without.

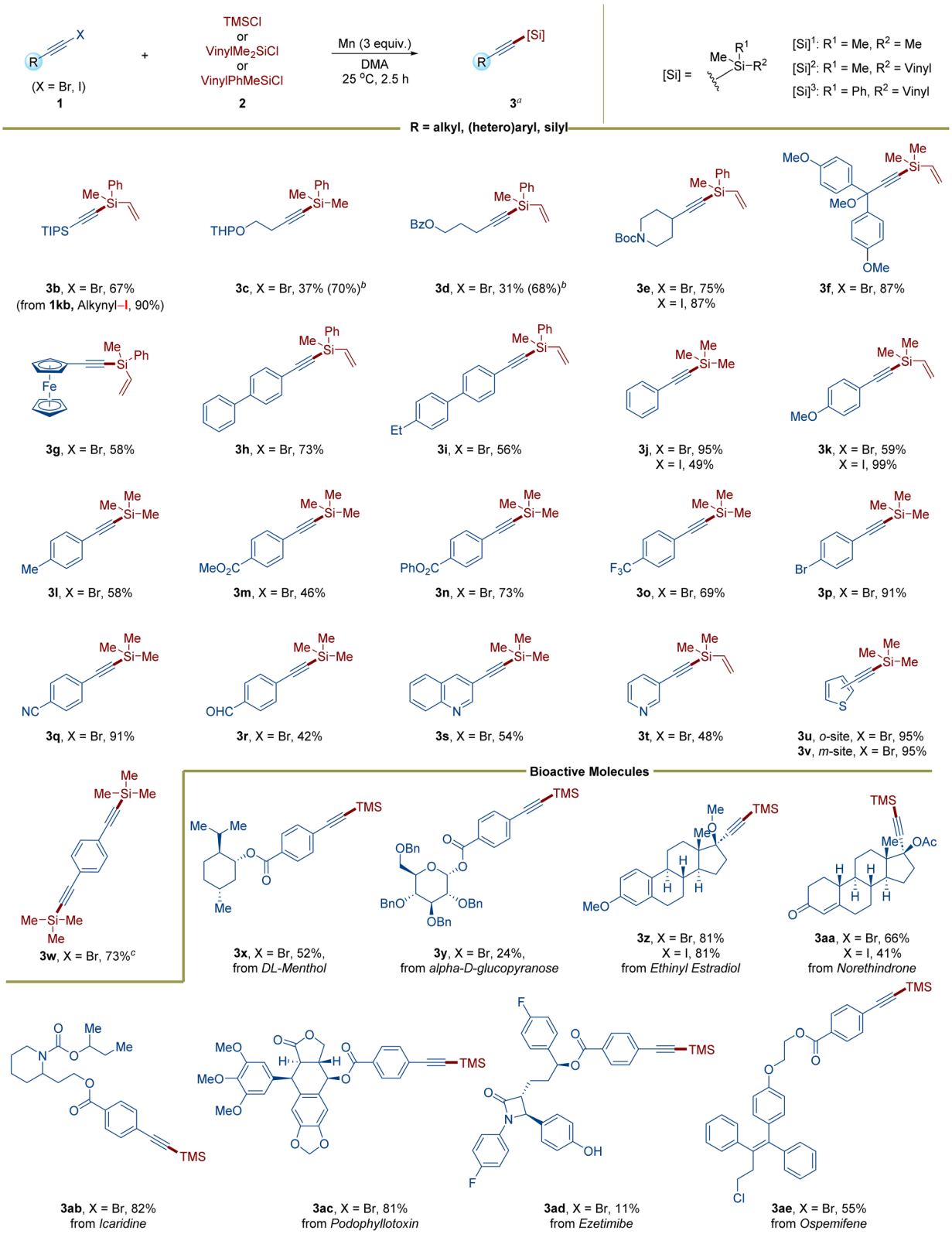

Fig. 2 Scope of alkynyl halides. [a] Reaction conditions: **1** (0.15 mmol), **2** (0.45 mmol), Mn (0.45 mmol), DMA (1 mL), 25 °C, Argon, isolated yield. [b] Chlorosilane (0.75 mmol) and Mn (0.75 mmol) were used, 48 h. [c] 0.6 mmol **2** and 0.6 mmol Mn were used.

while maintaining the integrity of their functional groups. Reactions involving aromatic alkynyl bromides with heteroaromatic rings proceeded smoothly, yielding alkynylsilanes (**3s**–**3v**) in yields of 48% to 95%. Furthermore, by increasing the amount of chlorosilanes, the bisilylation product **3w** was obtained with a yield of 73%. In certain cases, silica-based drug

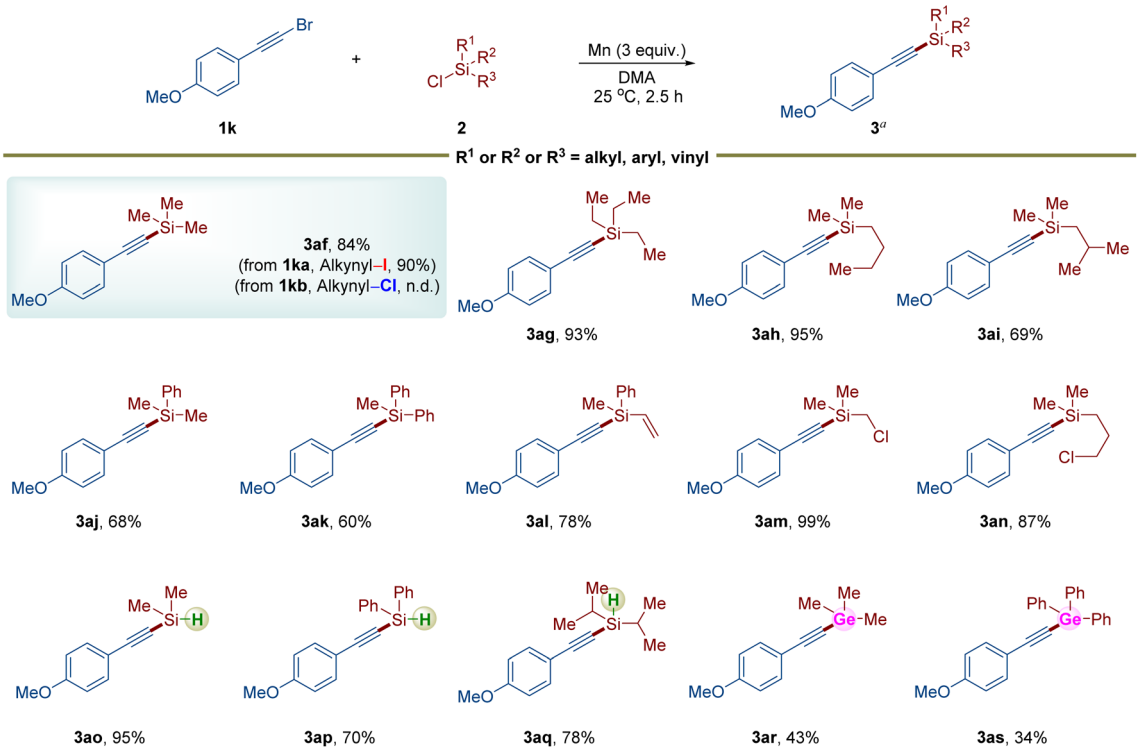

Fig. 3 The scope of alkynyl chlorosilanes. Reaction conditions: **1k** (0.15 mmol), **2** (0.45 mmol), Mn (0.45 mmol), DMA (1 mL), 25 °C, Argon, isolated yield. n.d. = not detected.

analogs exhibited superior pharmacokinetic properties.[12] We also explored the incorporation of alkynylsilane fragments into pharmaceutical and natural product scaffolds, including DL-menthol (**3x**), glycosides (**3y**), steroids (**3z–3aa**), icaridine (**3ab**), podophyllotoxin (**3ac**), ezetimibe (**3ad**), and ospemifene (**3ae**), achieving promising results. Additionally, when utilizing both unactivated and activated alkynyl iodides (**1ea**, **1ja**, **1ka**), as well as steroidal alkyne iodides (**1za**, **1aaa**), corresponding silylation products were obtained with yields ranging from 49% to 99%.

We subsequently examined the scope of chlorosilanes by coupling them with alkynyl bromide **1k** under standard conditions (Fig. 3). Depending on the varying chain lengths, steric properties, and functional groups of the chlorosilanes, we achieved yields ranging from good to excellent. For instance, TMSCl (**3af**), TESCl (**3ag**), chlorodimethyl(butyl)silane (**3ah**), and chlorodimethyl(isobutyl)silane (**3ai**) furnished the desired products in yields between 69% and 95%. Additionally, we assessed the compatibility of corresponding alkynyl halides under these conditions. Notably, alkynyl chloride (**1kb**) did not perform as anticipated, whereas alkynyl iodide (**1ka**) yielded product **3ab** with a 90% yield. Chlorosilanes bearing sterically hindered or conjugated functional groups, such as aryl and

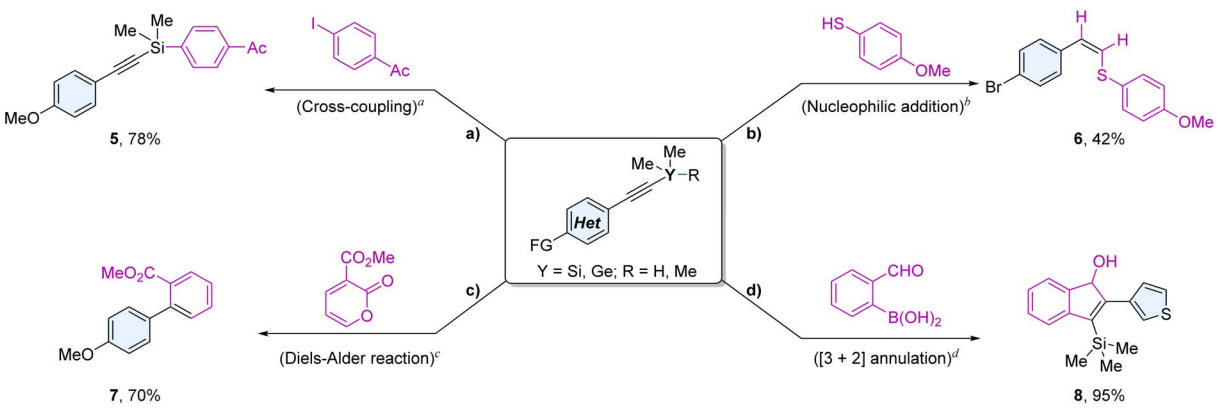

Fig. 4 Derivatization of alkynylsilanes/alkynylgermanes. Reaction conditions: [a] 1-(4-iodophenyl)ethan-1-one (0.15 mmol), **3ao** (2 equiv.), $Pd(OAc)_2$ (4 mol%), LiCl (4 equiv.), pyridine (2.4 equiv.), DMI, r.t. [b] **3p** (0.15 mmol), 4-methoxybenzenethiol (1 equiv.), KOH (1 equiv.), DMSO, 120 °C. [c] **3ar** (0.10 mmol), 2-pyrone (2 equiv.), $ZnCl_2$ (10 mol%), DCE, 140 °C. [d] **3v** (0.15 mmol), *ortho*-formylphenylboronic acid (1.5 equiv.), $Co(acac)_2$ (10 mol%), DPPE (10 mol%), MeCN, 80 °C.

alkenyl substituents (**3aj–3al**), resulted in target products with yields ranging from 60% to 78%. The incorporation of chloromethyl and chloropropyl functionalities onto the chlorosilanes was well tolerated, thus offering enhanced opportunities for late-stage modifications of the resultant products (**3am–3an**). Chlorohydrosilanes represent a fundamental class of materials in organosilicon chemistry.[8c,13] Previous studies have shown that the bond dissociation energy of Si–H (*ca.* 77 kcal mol^{-1}) is significantly lower than that of the Si–Cl bond.[14] Products **3ao–3aq** further illustrate that chlorohydrosilanes exhibit

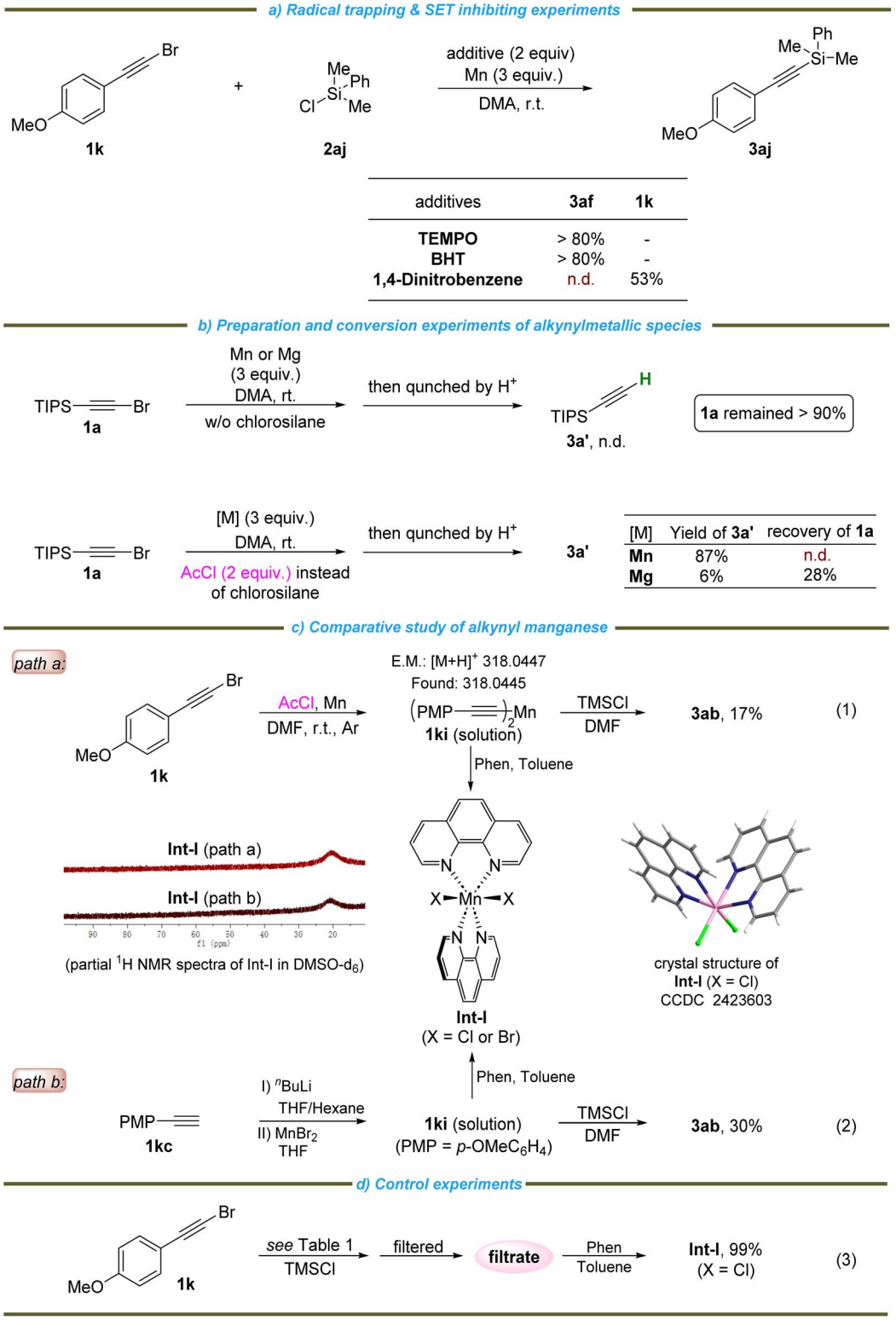

Fig. 5 Experiments designed to elucidate the reaction mechanism.

remarkable chemical selectivity under standard conditions. Moreover, the present method is also applicable to chlorogermanes, as demonstrated by examples **3ar** and **3as**.

The versatility of alkynylsilane functionality enables further structural variations (Fig. 4). The synthesized **3ao** derivatives are readily accessible for cross-coupling reactions, exemplified by the formation of compound **5**, which was obtained in 78% yield from the reaction of **3ao** with methyl 4-vinylbenzoate and 1-(4-iodophenyl)ethan-1-one.[15] In the nucleophilic addition of 4-methoxybenzenethiol to **3p**, product **6** is preferentially formed, yielding 42% and demonstrating exceptional chemical selectivity.[16] Additionally, alkynylgermane **3ar** undergoes a Diels–Alder reaction with 2-pyrones to afford biphenyl compound **7** in a yield of 70%, accompanied by the cleavage of the trimethylgermyl group.[17] Furthermore, a cobalt-catalyzed regioselective [3 + 2] annulation of **3v** with *ortho*-formylphenylboronic acid produced cyclized product **8** in a remarkable yield of 95%.[18] These compounds hold significant promise in biomedical applications and organic synthesis.[5a,19]

To elucidate the mechanism underlying this process, several control experiments were conducted. Firstly, in the presence of Michael acceptors **4a–4f** (3 equivalents), the reactions proceeded effectively, yielding the desired products with results ranging from 56% to 89%. Notably, no radical trapping product **9** was observed (see Scheme S1†). Furthermore, radical capture and inhibition experiments involving the addition of TEMPO and BHT to the silylation reaction demonstrated no significant effect on the formation of the desired product. In contrast, the introduction of 1,4-dinitrobenzene, a known single-electron transfer (SET) inhibitor, completely inhibited the reaction (Fig. 5a), indicating that the SET process may be involved in the oxidative addition of alkynyl bromide with active manganese (Mn*). Secondly, when the reaction was quenched with HCl (1 M, aqueous), no hydrogenation products were detected in the absence of chlorosilane, and nearly all of reactant **1a** was remained (Fig. 5b, top). Substituting AcCl (2 equiv.) for chlorosilane yielded the hydrogenated product in 87% yield with Mn as the reductant, while the yield decreased to 6% with Mg, leaving a surplus of 28% of reactant **1a** (Fig. 5b, bottom). The decomposition of chlorosilane in the reaction milieu Mn* facilitates the formation of the alkynylmanganese reagent.[5b,20] Thirdly, to identify the type of alkynylmanganese reagent involved in this reaction, the **1ki** solution generated from **1k** and manganese activated with acyl chloride was analyzed by LC-HRMS (Fig. 5c, eqn (1)). The results corresponded with the di(alkynyl)manganese species (HRMS data: exact mass $[M + H]^+$: 318.0447, found: 318.0445). This **1ki** solution was subsequently reacted with TMSCl, resulting in the formation of **3ab** with a yield of 17% (Fig. 5c, eqn (1)). Alternatively, **1ki** was synthesized through a previously established transmetallation of an acetylene lithium reagent with $MnBr_2$, followed by reaction with TMSCl, yielding **3ab** with a yield of 30% (Fig. 5c, eqn (2)). To

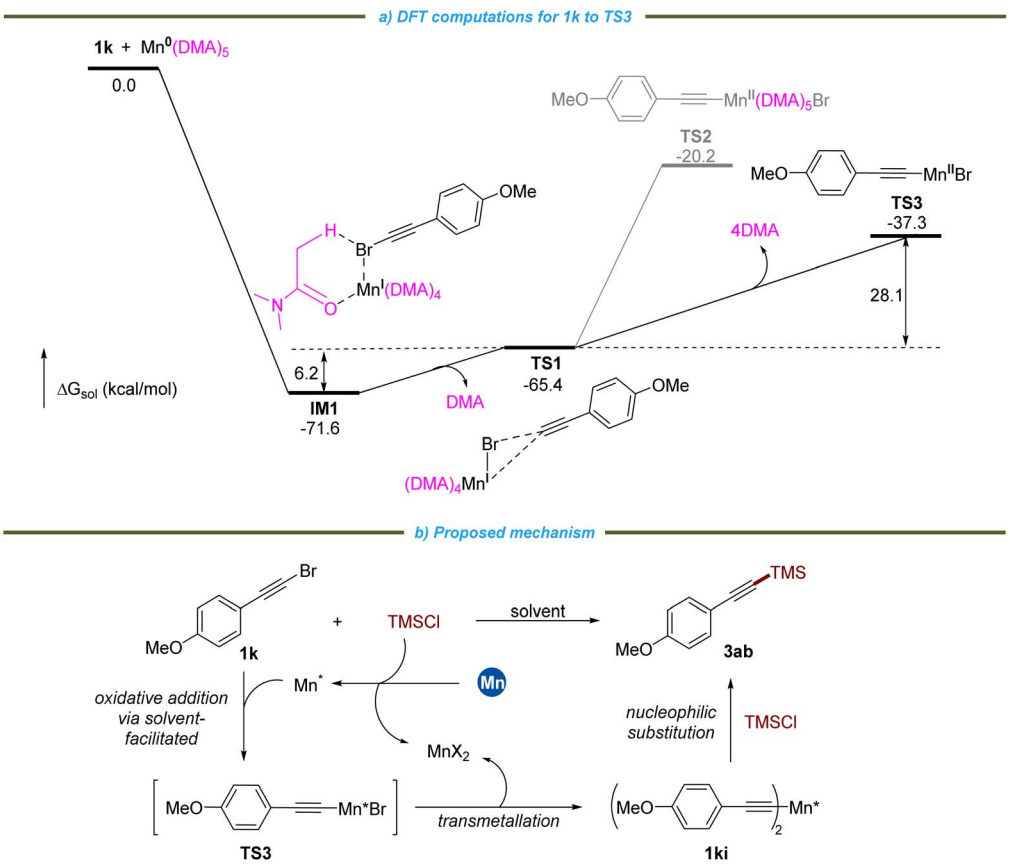

Fig. 6 DFT computations and proposed mechanism.

isolate or trap the di(alkynyl)manganese species **1ki**, 1,10-phenanthroline (Phen) was added. Upon the addition of Phen to the **1ki** solution formed *via* both pathways, an intermediate (**Int-I**) precipitated from the solution, with both exhibiting consistent paramagnetic NMR spectra. Unfortunately, the X-ray structure of **Int-I** was not identified as a di(alkynyl)manganese species; rather, it corresponded to $(Phen)_2MnCl_2$ (Fig. 5c). We speculate that the formation of MnX_2 occurs concurrently with the generation of the di(alkynyl)manganese species or stems from the activation of manganese with acyl chloride or TMSCl. Furthermore, results from the control experiments show that after the coupling of **1k** with TMSCl under standard conditions, the filtrate remains suitable for the synthesis of **Int-I** (X = Cl), indicating that a significant amount of $MnCl_2$ is produced during the reaction.[21]

Based on these experimental results and previous reports,[3,4,9a,12] a reaction pathway is illustrated in Fig. 6b. Alkyne bromide **1k** reacts with Mn* through an oxidative addition mechanism that involves a solvent-facilitated process, resulting in the formation of alkynylMn(II) bromide **TS3**. This is subsequently followed by transmetallation to yield **1ki**, accompanied by the generation of MnX_2.[22] The nucleophilic substitution of **1ki** with chlorosilanes produces the desired product, and the reaction pathway *via* **TS3** with chlorosilanes is ruled out.[23] Density Functional Theory (DFT) computations from **1k** to **TS3** provide support for this mechanistic proposal (Fig. 6a).[21] Our calculations indicate a significant decrease in free energy of 71.6 kcal mol^{-1} as the $Mn(DMA)_5$ complex[24] binds to the bromine atom of **1k** *via* a SET process, forming the highly stable intermediate **IM1**, which features a prominent six-membered ring with notable hydrogen bonding between the DMA and Br atoms. This finding underscores the indispensable role of amide solvents in facilitating this reaction (Table 1 and Fig. 6a). The reductive Mn(I) complex interacting with the electron-accepting compound **1k** leads to the formation of a three-membered transition state **TS1**, accompanied by the dissociation of a DMA molecule, requiring a moderate energy barrier of 6.2 kcal mol^{-1}. To achieve the transition state **TS3**, the synergistic process includes the dissociation of multiple DMA molecules and necessitates overcoming an additional energy barrier of 28.1 kcal mol^{-1}, which represents the rate-determining step of the entire reaction. DFT computations suggest that if the synergistic process fails to facilitate the dissociation of DMA, a less stable transition state **TS2** would form, requiring the overcoming of a higher energy barrier, thereby rendering this pathway unfavorable.

Conclusions

In summary, we have developed a novel method that enables the direct construction of C(sp)–Si bonds from alkynyl halides and chlorosilanes. This study marks the first reported XEC reaction mediated by the *in situ*-generated alkynylmanganese species, which subsequently engage in S_N2 reactions with electrophilic chlorosilanes. Density Functional Theory (DFT) computations highlight the pivotal role of amide solvents in facilitating the formation of these key alkynylmanganese intermediates. This protocol exhibits a broad substrate scope under mild reaction conditions, tolerating various aliphatic and aromatic alkynyl halides, as well as natural products and pharmaceutical-relevant molecules. The unique reactivity of alkynylsilanes offers diverse opportunities for late-stage derivatization and functionalization. Notably, our approach can also be extended to the XEC of alkynyl halides with chlorogermanes, and further explorations are currently being conducted in our laboratory. We expect to publish the progress in due course.

Data availability

All the data have been presented in the manuscript and ESI.†

Author contributions

QL, LL and JW performed the experiments. QL drafted the manuscript. DY, ZC and ZXW designed the project and revised the manuscript drafting. All the authors participated in the preparation of the manuscript.

Conflicts of interest

There are no conflicts to declare.

Acknowledgements

Financial support for this work from the National Natural Science Foundation of China (No. 22222502, 22301043, 22462001) is gratefully acknowledged, and the Gannan Normal University Start-up Fund (No. BSJJ202306). This research was also supported by the Research Team Program of Gannan Normal University. We also thank Ye Xu from SINAP for assisting us in the growth of crystals.

Notes and references

1 For selected reviews and examples about recent efforts to cross-electrophile coupling, see: (*a*) W. L. Williams, N. E. Gutiérrez-Valencia and A. G. Doyle, *J. Am. Chem. Soc.*, 2023, **145**, 24175–24183; (*b*) D. A. Everson and D. J. Weix, *J. Org. Chem.*, 2014, **79**, 4793–4798; (*c*) J. Liu, Y. Ye, J. L. Sessler and H. Gong, *Acc. Chem. Res.*, 2020, **53**, 1833–1845; (*d*) Q. Pan, K. Wang, W. Xu, Y. Ai, Y. Ping, C. Liu, M. Wang, J. Zhang and W. Kong, *J. Am. Chem. Soc.*, 2024, **146**, 15453–15463; (*e*) D. J. Weix, *Acc. Chem. Res.*, 2015, **48**, 1767–1775; (*f*) J. Duan, Y.-F. Du, X. Pang and X.-Z. Shu, *Chem. Sci.*, 2019, **10**, 8706–8712; (*g*) H. Meng, J.-S. Jia, P.-F. Yang, Y.-L. Li, Q. Yu and W. Shu, *Chem. Sci.*, 2025, **16**, 4442–4449; (*h*) D. Sun, G. Ma, X. Zhao, C. Lei and H. Gong, *Chem. Sci.*, 2021, **12**, 5253–5258; (*i*) Y. Ye, X. Qi, B. Xu, Y. Lin, H. Xiang, L. Zou, X.-Y. Ye and T. Xie, *Chem. Sci.*, 2022, **13**, 6959–6966; (*j*) K. E. Poremba, S. E. Dibrell and S. E. Reisman, *ACS Catal.*, 2020, **10**, 8237–8246; (*k*) A. Tortajada, M. Börjesson and R. Martin, *Acc. Chem. Res.*, 2021, **54**, 3941–3952; (*l*) J. Gu, X. Wang, W. Xue and H. Gong, *Org. Chem. Front.*, 2015, **2**, 1411–1421; (*m*) Z. Wu,

H. Jiang and Y. Zhang, *Chem. Sci.*, 2021, **12**, 8531–8536; (*n*) L. M. Kammer, S. O. Badir, R.-M. Hu and G. A. Molander, *Chem. Sci.*, 2021, **12**, 5450–5457; (*o*) E. Richmond and J. Moran, *Synthesis*, 2018, **50**, 499–513; (*p*) C. E. I. Knappke, S. Grupe, D. Gärtner, M. Corpet, C. Gosmini and A. Jacobi von Wangelin, *Chem.–Eur. J.*, 2014, **20**, 6828–6842.

2 (*a*) T. Hiyama, M. Obayashi and A. Nakamura, *Organometallics*, 1982, **1**, 1249–1251; (*b*) S.-H. Kim and R. D. Rieke, *Synth. Commun.*, 1998, **28**, 1065–1072; (*c*) S.-H. Kim and R. D. Rieke, *J. Org. Chem.*, 1998, **63**, 6766–6767; (*d*) G. Cahiez, A. Martin and T. Delacroix, *Tetrahedron Lett.*, 1999, **40**, 6407–6410; (*e*) G. Cahiez, C. Duplais and J. Buendia, *Chem. Rev.*, 2009, **109**, 1434–1476; (*f*) G. Dagousset, C. François, T. León, R. Blanc, E. Sansiaume-Dagousset and P. Knochel, *Synthesis*, 2014, **46**, 3133–3171; (*g*) W. Yan, A. T. Poore, L. Yin, S. Carter, Y.-S. Ho, C. Wang, S. C. Yachuw, Y.-H. Cheng, J. A. Krause, M.-J. Cheng, S. Zhang, S. Tian and W. Liu, *J. Am. Chem. Soc.*, 2024, **146**, 15176–15185; (*h*) D. Knyszek, J. Löffler, D. E. Anderson, E. Hevia and V. H. Gessner, *J. Am. Chem. Soc.*, 2025, **147**, 5417–5425; (*i*) A. H. Cherney, N. T. Kadunce and S. E. Reisman, *Chem. Rev.*, 2015, **115**, 9587–9652; (*j*) X. Hu, *Chem. Sci.*, 2011, **2**, 1867–1886.

3 (*a*) J. Duan, K. Wang, G.-L. Xu, S. Kang, L. Qi, X.-Y. Liu and X.-Z. Shu, *Angew. Chem., Int. Ed.*, 2020, **59**, 23083–23088; (*b*) P.-F. Su, K. Wang, X. Peng, X. Pang, P. Guo and X.-Z. Shu, *Angew. Chem., Int. Ed.*, 2021, **60**, 26571–26576; (*c*) P. Guo, X. Pang, K. Wang, P.-F. Su, Q.-Q. Pan, G.-Y. Han, Q. Shen, Z.-Z. Zhao, W. Zhang and X.-Z. Shu, *Org. Lett.*, 2022, **24**, 1802–1806; (*d*) X. Pang, P.-F. Su and X.-Z. Shu, *Acc. Chem. Res.*, 2022, **55**, 2491–2509; (*e*) Y.-H. Yang, X. Pang and X.-Z. Shu, *Synthesis*, 2022, **55**, 868–876; (*f*) X. Pang and X.-Z. Shu, *Chem.–Eur. J.*, 2023, **29**, e202203362; (*g*) G.-Y. Han, P.-F. Su, Q.-Q. Pan, X.-Y. Liu and X.-Z. Shu, *Nat. Catal.*, 2024, **7**, 12–20; (*h*) C. Li, S. Yang and X. Zeng, *ACS Catal.*, 2023, **13**, 12062–12073; (*i*) Y. Lin, L. Zou, R. Bai, X.-Y. Ye, T. Xie and Y. Ye, *Org. Chem. Front.*, 2023, **10**, 3052–3060; (*j*) J. Manigrasso, I. Chillón, V. Genna, P. Vidossich, S. Somarowthu, A. M. Pyle, M. De Vivo and M. Marcia, *Nat. Commun.*, 2022, **13**, 1.

4 D. Xing, J. Liu, D. Cai, B. Huang, H. Jiang and L. Huang, *Nat. Commun.*, 2024, **15**, 4502.

5 (*a*) W. Wu and H. Jiang, *Acc. Chem. Res.*, 2014, **47**, 2483–2504; (*b*) L. Huang, A. M. Olivares and D. J. Weix, *Angew. Chem., Int. Ed.*, 2017, **56**, 11901–11905; (*c*) R. Pan, C. Shi, D. Zhang, Y. Tian, S. Guo, H. Yao and A. Lin, *Org. Lett.*, 2019, **21**, 8915–8920; (*d*) Y. Jiang, J. Pan, T. Yang, Y. Zhao and M. J. Koh, *Chem*, 2021, **7**, 993–1005.

6 (*a*) J. Z. Dávalos and T. Baer, *J. Phys. Chem. A*, 2006, **110**, 8572–8579; (*b*) L. Lu, J. C. Siu, Y. Lai and S. Lin, *J. Am. Chem. Soc.*, 2020, **142**, 21272–21278; (*c*) H. Yoo, P. J. Carroll and D. H. Berry, *J. Am. Chem. Soc.*, 2006, **128**, 6038–6039; (*d*) L. Qiu, Y. Liu, H. Chen, L. Song and W. Xie, *Chem. Sci.*, 2025, **16**, 9454–9461.

7 (*a*) C.-L. Ji, X. Zhai, Q.-Y. Fang, C. Zhu, J. Han and J. Xie, *Chem. Soc. Rev.*, 2023, **52**, 6120–6138; (*b*) S. Jin, H. T. Dang, G. C. Haug, R. He, V. D. Nguyen, V. T. Nguyen, H. D. Arman, K. S. Schanze and O. V. Larionov, *J. Am. Chem. Soc.*, 2020, **142**, 1603–1613; (*c*) T. Xiao-Jun and C. Qing-Yun, *Chem. Sci.*, 2012, **3**, 1694–1697.

8 (*a*) J. Duan, Y. Wang, L. Qi, P. Guo, X. Pang and X.-Z. Shu, *Org. Lett.*, 2021, **23**, 7855–7859; (*b*) L. Zhang and M. Oestreich, *Angew. Chem., Int. Ed.*, 2021, **60**, 18587–18590; (*c*) Z.-Z. Zhao, X. Pang, X.-X. Wei, X.-Y. Liu and X.-Z. Shu, *Angew. Chem., Int. Ed.*, 2022, **61**, e202200215.

9 (*a*) L. Qi, X. Pang, K. Yin, Q.-Q. Pan, X.-X. Wei and X.-Z. Shu, *Chin. Chem. Lett.*, 2022, **33**, 5061–5064; (*b*) V. Lanke and I. Marek, *Chem. Sci.*, 2020, **11**, 9378–9385.

10 (*a*) A. Fürstner and H. Brunner, *Tetrahedron Lett.*, 1996, **37**, 7009–7012; (*b*) S.-H. Kim, M. V. Hanson and R. D. Rieke, *Tetrahedron Lett.*, 1996, **37**, 2197–2200; (*c*) H. Kakiya, S. Nishimae, H. Shinokubo and K. Oshima, *Tetrahedron*, 2001, **57**, 8807–8815; (*d*) P. DeShong, D. R. Sidler, P. J. Rybczynski, G. A. Slough and A. L. Rheingold, *J. Am. Chem. Soc.*, 1988, **110**, 2575–2585; (*e*) R. Takahashi, P. Gao, K. Kubota and H. Ito, *Chem. Sci.*, 2023, **14**, 499–505.

11 (*a*) C. J. Elsevier, H. Kleijn, J. Boersma and P. Vermeer, *Organometallics*, 1986, **5**, 716–720; (*b*) A. J. Eberhart, H. J. Shrives, E. Álvarez, A. Carrër, Y. Zhang and D. J. Procter, *Chem.–Eur. J.*, 2015, **21**, 7428–7434; (*c*) P. B. Changala, P. R. Franke, J. F. Stanton, G. B. Ellison and M. C. McCarthy, *J. Am. Chem. Soc.*, 2024, **146**, 1512–1521.

12 A. A. Toutov, K. N. Betz, D. P. Schuman, W.-B. Liu, A. Fedorov, B. M. Stoltz and R. H. Grubbs, *J. Am. Chem. Soc.*, 2017, **139**, 1668–1674.

13 (*a*) M.-M. Liu, Y. Xu and C. He, *J. Am. Chem. Soc.*, 2023, **145**, 11727–11734; (*b*) Y. Ge, J. Ke and C. He, *Acc. Chem. Res.*, 2025, **58**, 375–398; (*c*) Y. Wu, L. Zheng, Y. Wang and P. Wang, *Chem*, 2023, **9**, 3461–3514.

14 (*a*) R. Tacke and U. Wannagat, Bioactive Organo-Silicon Compounds, *Topics in Current Chemistry*, Vol. 84, Springer, Berlin, Heidelberg, 1979; (*b*) T. Liu, X.-R. Mao, S. Song, Z.-Y. Chen, Y. Wu, L.-P. Xu and P. Wang, *Angew. Chem., Int. Ed.*, 2023, **62**, e202216878.

15 A. Hamze, O. Provot, M. Alami and J.-D. Brion, *Org. Lett.*, 2006, **8**, 931–934.

16 M. Patel, R. K. Saunthwal, D. K. Dhaked, P. V. Bharatam and A. K. Verma, *Asian J. Org. Chem.*, 2015, **4**, 894–898.

17 M.-M. Xu, X.-Y. You, Y.-Z. Zhang, Y. Lu, K. Tan, L. Yang and Q. Cai, *J. Am. Chem. Soc.*, 2021, **143**, 8993–9001.

18 M. Ueda, T. Ueno, Y. Suyama and I. Ryu, *Tetrahedron Lett.*, 2017, **58**, 2972–2974.

19 (*a*) M. Suginome and Y. Ito, *Chem. Rev.*, 2000, **100**, 3221–3256; (*b*) R. Ramesh and D. S. Reddy, *J. Med. Chem.*, 2018, **61**, 3779–3798; (*c*) J. Zhu, S. Chen and C. He, *J. Am. Chem. Soc.*, 2021, **143**, 5301–5307.

20 (*a*) K. Takai, T. Ueda, T. Hayashi and T. Moriwake, *Tetrahedron Lett.*, 1996, **37**, 7049–7052; (*b*) S. Biswas and D. J. Weix, *J. Am. Chem. Soc.*, 2013, **135**, 16192–16197; (*c*) K. A. Johnson, S. Biswas and D. J. Weix, *Chem.–Eur. J.*, 2016, **22**, 7399–7402; (*d*) M. Xü, S. Wu and G. Zou, *Eur. J. Org Chem.*, 2024, **27**, e202400625; (*e*) K. E. Poremba, N. T. Kadunce, N. Suzuki, A. H. Cherney and S. E. Reisman, *J. Am. Chem. Soc.*, 2017, **139**, 5684–5687.

21 See the ESI† for details.
22 (*a*) M. Tamura and J. Kochi, *J. Organomet. Chem.*, 1971, **29**, 111–129; (*b*) I. Suzuki, M. Yasuda and A. Baba, *Chem. Commun.*, 2013, **49**, 11620–11622.
23 (*a*) R. West and L. C. Quass, *J. Organomet. Chem.*, 1969, **18**, 55–67; (*b*) S. HariPrasad and G. Nagendrappa, *Tetrahedron*, 1993, **49**, 3387–3396; (*c*) M. Kunishima, D. Nakata, S. Tanaka, K. Hioki and S. Tani, *Tetrahedron*, 2000, **56**, 9927–9935.
24 (*a*) G. A. Carriedo, D. Miguel and V. Riera, *J. Organomet. Chem.*, 1988, **342**, 373–380; (*b*) J. Chai, H. Zhu, H. W. Roesky, Z. Yang, V. Jancik, R. Herbst-Irmer, H.-G. Schmidt and M. Noltemeyer, *Organometallics*, 2004, **23**, 5003–5006; (*c*) D. Unseld, V. V. Krivykh, K. Heinze, F. Wild, G. Artus, H. Schmalle and H. Berke, *Organometallics*, 1999, **18**, 1525–1541; (*d*) V. V. Krivykh, I. L. Eremenko, D. Veghini, I. A. Petrunenko, D. L. Pountney, D. Unseld and H. Berke, *J. Organomet. Chem.*, 1996, **511**, 111–114.